Coherent-potential approximation for the lattice vibrations of mixed diatomic systems*

P. N. Sen† and W. M. Hartmann
Michigan State University, East Lansing, Michigan 48823
(Received 8 August 1973)

We generalize the coherent-potential approximation (CPA) for the lattice dynamics of mass-disordered systems to the case of mixed diatomic crystals. Specific results are obtained for a one-dimensional model. We prove that for mass defects on only one sublattice the CPA self-energy is nonzero only on that sublattice. We compare the configuration-averaged density of states calculated by the CPA with computer experiments on several mixed diatomic chains. We compare the CPA dielectric susceptibility for the one-dimensional model with the experimental optical properties of several interesting III-V, II-VI, and I-VII mixed crystals. With some qualifications we conclude that the CPA in one-dimension can explain the switching from one-mode- to two-mode-type behavior observed in some III-V mixed systems and unexplained by previous theories. Finally, we present a one-dimensional CPA phase diagram for the transition from one optic band to two optic bands in the density of states.

I. INTRODUCTION

The infrared spectra of mixed diatomic crystals of the form $AB_{1-c}C_c$ have been the subject of a great deal of experimental and theoretical work. A recent review has been given by Chang and Mitra.[1] Typically the observed infrared- or Raman-active modes in the mixed crystals have been categorized according to two classes, one-mode or amalgamation type and two-mode or persistent type. In one-mode systems the infrared-active band varies continuously with composition from the characteristic frequencies of one end member to frequencies of the other, with the strength of the band remaining approximately constant. Examples of this type of mixed crystal are $K_{1-c}Na_cCl$, $Rb_{1-c}K_cCl$, $Tl_{1-c}K_cCl$, $Cd_{1-c}Zn_cS$, and $ZnTe_{1-c}Se_c$. In the two-mode type, two bands of frequencies, close to those of the individual diatomic components, persist in the mixed crystal. The strength of each band grows from zero to the maximum as the concentration of the corresponding constituent is increased. Examples of this kind are $Rb_{1-c}K_cI$, $ZnSe_{1-c}S_c$, and $Ga_{1-c}Al_cAs$.

Some mixed crystals, however, appear to switch from one-mode to two-mode behavior as the composition is changed. These are III-V systems, $In_{1-c}Ga_cSb$, $In_{1-c}Ga_cAs$, $GaSb_{1-c}As_c$, and $InSb_{1-c}As_c$. For example, $In_{1-c}Ga_cSb$ is one-mode for $c > 0.7$; for smaller c it is two-mode.[2]

There have been numerous attempts to provide a theoretical criterion for predicting one- or two-mode behavior. These too have been reviewed by Chang and Mitra. Of these we note just several. In the modified-random-element-isodisplacement (MREI) model it is assumed that all anion-cation pairs of the crystal vibrate in phase, as in the $k = 0$ optic mode of a perfect diatomic crystal. This leads to a criterion for two-mode behavior depending only on the masses of the constituents,[3]

$$M_C^{-1} > M_A^{-1} + M_B^{-1}. \tag{1}$$

This theory is further discussed in Sec. V.

A second criterion is that of Lucovsky, Brodsky, and Burstein.[4] These authors first propose a method whereby local-mode formation in three-dimensional systems may be predicted from a one-dimensional model. They then argue that a mixed system should show two-mode behavior if a local mode exists in the limit of small concentration of the light constituent. This theory is discussed further in Sec. IV B.

The recent theoretical criteria for one-mode–two-mode behavior are based upon the nature of the systems in the limit of vanishing concentration of one or more constituents. Therefore, none of these theories is concentration dependent. By considering both high- and low-concentration limits one might find a criterion for systems which switch from one-mode to two-mode types.[5] However, such a theory will not be able to predict the concentration at which the transition occurs.

In this paper we present a theory for a mixed diatomic system, which is valid at all compositions. Because this disordered-system problem cannot be solved exactly, we employ a self-consistent-field approach which has been called the coherent-potential approximation (CPA). The CPA was developed by Taylor[6] and by Soven[7] for disordered binary alloys. Among its many virtues the CPA is able to predict transitions from single-band to split-band behavior in disordered systems.[8] It is then natural to try to apply this method to the problem of mixed diatomic systems. In order to study the systematics of the CPA for mixed diatomic systems we chose a simple model, a one-dimensional chain with mass defects on one of two sublattices. This one-dimensional model includes the most important features of the three-dimensional system and has often been used to discuss

the optical properties of real systems.[9] We note that Taylor has very recently applied the CPA to three-dimensional calculations of the susceptibility for several mixed alkali halides.[10] Such calculations involve considerably more numerical effort than do our one-dimensional calculations, for which we can find analytic expressions for the perfect Green's functions.

In Sec. II we present the one-dimensional model and introduce the Green's functions for a perfect diatomic chain. In Sec. III we first apply the Green's functions to review the single-defect problem, which corresponds to the low-concentration limit of the CPA. We then develop the CPA for a mixed diatomic system. In particular, we show in the Appendix that for mass defects on only one sublattice the self-energy is nonzero only on that sublattice. We further develop the expressions for the configuration-averaged density of states and dielectric susceptibility. In Sec. III we first compare the CPA theory for the density of states with the spectra of mixed diatomic chains produced by computer experiment. We next compare the CPA susceptibility with the experimental optical properties of III-V, II-VI, and I-VII mixed crystals. In Sec. V we present concentration-dependent phase boundaries delimiting the regimes of one-band and two-band behavior for the CPA density of states for the mixed diatomic chain.

II. DIATOMIC MODEL

Our model system is a harmonic linear chain with nearest-neighbor atoms, separated by distance $\frac{1}{2}a$, connected by force constants f. Let $u_{l\alpha}$ be the displacement from equilibrium of the atom of mass $M_{l\alpha}$ on the sublattice α in the lth unit cell. The equation of motion is

$$M_{l\alpha}\omega^2 u_{l\alpha} = \sum_{l'\beta} A_{ll'\alpha\beta} u_{l'\beta} \quad , \tag{2}$$

where $\underline{A}$ is the appropriate force-constant matrix.

We shall be concerned with Green's functions which are basically the thermal average of the commutator of displacement operators at different times.[11] Generally,

$$G_{ll'\alpha\beta}(t) = \frac{2\pi}{i\hbar}\,\theta(t) \times \langle [u_{l\alpha}(\tau+t),\ u_{l'\beta}(\tau)] \rangle \tag{3}$$

for any disordered system. Our approach is to find a solution or an approximate solution for $\vec{G}$ in terms of a perfect diatomic chain of alternating masses, M_H (heavy) and M_L (light). The remainder of this section deals with the properties of such a perfect diatomic chain.

For the perfect periodic chain we may write the displacements in terms of the eigenvectors for normal modes of branch j (j being acoustic or optic) and wave vector k.

$$M_\alpha^{1/2} u_{l\alpha} \equiv v_{l\alpha} = \sum_{jk} \sigma_\alpha^j(k) e^{ikR_l} \quad , \tag{4}$$

where R_l is the position of the lth unit cell and

$$x_j(k)\sigma_\alpha^j(k) = \sum_{\beta=H,L} A_{\alpha\beta}(k)\sigma_\beta^j(k) \quad . \tag{5}$$

Here $\underline{A}(k)$ is the dynamical matrix and $x_j(k)$ $[\equiv \omega_j^2(k)]$ is the eigenvalue, the square of the angular frequency.[12] The dispersion relation is given by

$$x_j(k) = \tfrac{1}{2}X_T \pm \tfrac{1}{2}\left[X_T^2 - 4X_A X_O \times \sin^2 \tfrac{1}{2}ka\right]^{1/2} \quad , \tag{6}$$

where the maximum frequency X_T and acoustic and optic zone-boundary frequencies, X_A and X_O, are shown in Fig. 1. For the acoustic branch ($j=A$) the minus sign applies, for the optic branch ($j=O$) the plus sign applies, and for any k, $X_A(k)+X_O(k) = X_T$.

The density of states $g(x)$, also shown in Fig. 1, is

$$g(x) = \mathrm{Re}\,(1/\pi)\,|X_T - 2x| \times [(X_T - x)(x - X_O)(x - X_A)\,x]^{-1/2} \quad . \tag{7}$$

The density of states is symmetric about the center of the gap at $\frac{1}{2}X_T$ and is normalized,

$$\int_0^\infty g(x)\,dx = 2 \quad . \tag{8}$$

The orthonormalized eigenvectors are given by

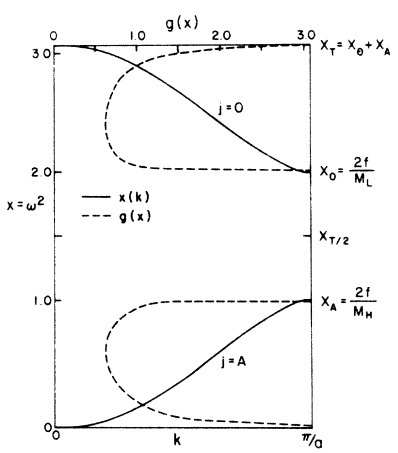

FIG. 1. Dispersion relation $x_j(k)$ (—) and the density of states $g(x)$ (---) for the periodic alternating diatomic chain with nearest-neighbor forces. For this example, $f=1$, $M_H=2$, and $M_L=1$. The area under $g(x)$ is equal to 2.

$$\sigma_1^j(k) = \left(\frac{x_j(k) - X_2}{2x_j(k) - X_T}\right)^{1/2} , \tag{9a}$$

$$\sigma_2^j(k) = \tfrac{1}{2}\frac{(X_1X_2)^{1/2}}{X_2 - x_j(k)} \times (1 + e^{-ika})\,\sigma_1^j(k) , \tag{9b}$$

where labels 1 and 2 on σ stand for sublattices 1 and 2 with masses M_1 and M_2, respectively. The zone-boundary squared frequencies are $X_1 \equiv 2f/M_1$ and $X_2 \equiv 2f/M_2$. The assignment of M_1 and M_2 to heavy and light atoms of the perfect chain is arbitrary.

For the perfect diatomic chain the Green's function of Eq. (3) is called $\underline{P}$. The Fourier transform of the retarded $\underline{P}$ is given by

$$P_{ll'\alpha\beta}(x) = \lim_{\phi\to 0+}\frac{1}{N}(M_\alpha M_\beta)^{-1/2} \times \sum_{jk}\frac{\sigma_\alpha^{j*}(k)\sigma_\beta^j(k)}{x - x_j(k) + i\phi} \times e^{-ik(R_l - R_{l'})} , \tag{10}$$

where N is the number of unit cells.

Using Eq. (9) and (6) and performing a contour integration, we find the diagonal parts of the Greens's functions in real space,

$$P_{ll\,11}(x) \equiv \frac{1}{N}\sum_k P_{11}(k,x) = \frac{1}{NM_1}\sum_k \frac{x - X_2}{[x - x_A(k)][x - x_O(k)]} , \tag{11}$$

$$P_{ll\,11}(x) = \frac{x - X_2}{M_1}\,\frac{1}{x^{1/2}(x - X_A)^{1/2}(x - X_O)^{1/2}(x - X_T)^{1/2}} , \tag{12a}$$

$$P_{ll\,22}(x) = \frac{x - X_1}{x - X_2}\frac{M_1}{M_2}P_{ll\,11}(x) , \tag{12b}$$

and

$$P_{ll\,12}(x) = P^*_{ll\,21}(x) = -\frac{1}{2N}\left(\frac{X_1X_2}{M_1M_2}\right)^{1/2}\sum_k \frac{1 + e^{-ika}}{[x - x_A(k)][x - x_O(k)]} . \tag{12c}$$

Each square root in Eq. (12a) must be evaluated in the following way. If the argument of the square root is positive then the positive square root is taken. If the argument of the square root is negative then the positive imaginary root is taken. The real and imaginary parts of the diagonal real-space Green's functions, Eqs. (12a) and (12b), are plotted, in Fig. 2, as part of the discussion of the single-defect problem.

III. THEORY FOR A MIXED DIATOMIC CHAIN

In a mixed diatomic chain defects are substituted for host atoms on one of the two sublattices; the other sublattice is unchanged from the perfect chain. We adopt the notational convention that the defective sublattice is sublattice No. 1. Therefore the following convention for subscripts α apply.

If the defects are on the sublattice of heavy-host atoms ($\beta > 1$),

$$1 = H \text{ and } X_1 \equiv 2f/M_1 = X_A , \qquad 2 = L \text{ and } X_2 \equiv 2f/M_2 = X_O . \tag{13a}$$

If the defects are on the sublattice of light-host atoms ($\beta < 1$),

$$1 = L \text{ and } X_1 \equiv 2f/M_1 = X_O , \qquad 2 = H \text{ and } X_2 \equiv 2f/M_2 = X_A . \tag{13b}$$

If defects of mass M_1' are substituted for a fraction c of the atoms on sublattice 1 the Green's function for the defective chain is given by the matrix equation[11]

$$\underline{G}(x) = \underline{P}(x) + \underline{P}(x)\,\underline{C}(x)\,\underline{G}(x) , \tag{14}$$

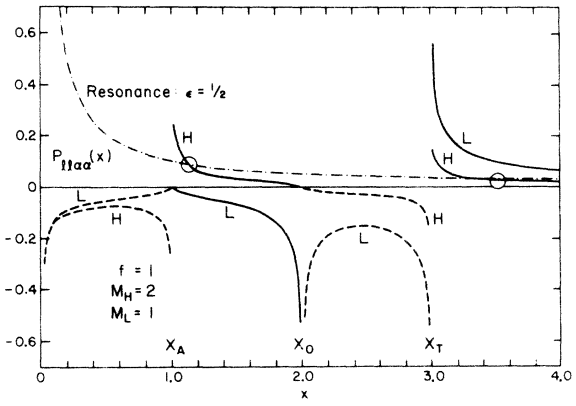

FIG. 2. Real (—) and imaginary (---) parts of the diagonal real-space perfect diatomic-chain Green's function $P_{llLL}(x)$ and $P_{llHH}(x)$ defined in Eq. (12). For this calculation $f = 1$, $M_H = 2$, and $M_L = 1$ as for Fig. 1. The dashed curve is the function $(\epsilon - xM_H)^{-1}$ for $\epsilon = 0.5$. The intersections of this curve with the real part of P_{llHH} (circles) give the gap and local-mode frequencies when a defect with mass equal to the mass of the light-host atoms is substituted for a heavy atom.

where $\underline{C}$ is a diagonal matrix in real-space coordinates with elements

$$C_{ll\,11} = (M_1 - M_1')\,x \equiv M_1\,\epsilon_{11}\,x \quad \text{if } l \text{ is a defect cell,}$$
$$C_{ll\,11} = 0 \quad \text{if } l \text{ is a host cell,} \tag{15}$$
$$C_{ll\,22} = 0 \quad \text{by definition .}$$

In addition to the parameter

$$\epsilon \equiv \epsilon_{11} \equiv 1 - M_1'/M_1 \ , \tag{16}$$

we introduce

$$\beta \equiv M_1/M_2 \ . \tag{17}$$

Before considering the theory valid for arbitrary c, it is instructive to review the single-defect problem. In the limit $c = 1/N$, any valid theory for arbitrary c must predict that physical quantities, such as the density of states, tend to the result predicted by the single-defect theory.

A. Single-defect theory

If there is only a single defect in the chain located in cell $l = 0$ on sublattice 1, the Dyson equation (14) for the imperfect-chain Green's function in a real-space representation becomes a 2×2 matrix equation which can be solved exactly,

$$\underline{G} = \underline{P} + \underline{P}\underline{T}\underline{P} \ , \tag{18}$$

$$T_{ll'\alpha\beta} = \delta_{l0}\delta_{l'0}\delta_{\alpha1}\delta_{\beta1}C_{0011} \times (1 - P_{0011}C_{0011})^{-1} \ . \tag{19}$$

Since the real part of P_{00} is zero inside the perfect-chain bands there are no resonance modes. Infinitely sharp local modes and gap modes occur at frequencies where the matrix $\underline{T}$ diverges. In particular, if the defect is put onto a heavy-atom ($\beta > 1$) site the divergence occurs if

$$1 - M_H \epsilon x \,\mathrm{Re} P_{00HH} = 0 \ ; \tag{20a}$$

if the defect is put onto a light-atom ($\beta < 1$) site the divergence occurs if

$$1 - M_L \epsilon x \,\mathrm{Re} P_{00LL} = 0 \ . \tag{20b}$$

Since ϵ is positive ($0 < \epsilon < 1$) if the defect has a mass smaller than that of the atom which it replaces, and since ϵ is negative ($-\infty < \epsilon < 0$) if the defect is heavier than the atom it replaces, Fig. 2 for the real part of the perfect chain Green's function illustrates the following well-known behavior.[13]

(a) [$\beta < 1$, $\epsilon > 0$]. If the light-host atom is replaced by a lighter one, then a local mode forms above X_T.

(b) [$\beta < 1$, $\epsilon < 0$]. If the light-host atom is replaced by a heavier one (which may be lighter or heavier than the heavy-host atom), then a gap mode peels off from the bottom of the optic band to frequency x_G, $X_A < x_G < X_O$.

(c) [$\beta > 1$, $\epsilon > 0$]. If the heavy-host atom is replaced by a lighter one (which may be lighter or heavier than the light-host atom), then both gap and local modes occur. The gap mode in this case rises from the top of the acoustic band with decreasing defect mass.

(d) [$\beta > 1$, $\epsilon < 0$]. If the heavy atom is replaced by a heavier atom, then no gap or local modes occur.

This theory of the single-defect problem is exact. For an arbitrary concentration of defects no exact solution to Eq. (14), has ever been evaluated; an approximate theory follows.

B. Coherent-potential approximation

For an arbitrary concentration of defects the distinction between "defect" and "host" atoms is arbitrary. In practice we shall define the defect as the lighter of the two atoms which may occupy sites on the defective (No. 1) sublattice. Therefore we always have $\epsilon > 0$. We find an approximate solution for a configuration-averaged Green's function $\overline{\underline{G}}$ by using a self-consistent-field approach introduced by Taylor and by Soven, and usually called the C. P. A. The essential nontrivial step in the theory to follow is the generalization of Taylor's self-consistent-field theory for lattice dynamics[6] to mixed diatomic systems.

This section is the most important part of the paper and fortunately most of it is valid for systems of n dimensions. Although we retain the notation of our one-dimensional problem the equations can be generalized by treating such quantities as $P_{ll\alpha\beta}$ as $n\times n$ matrices. The proof in the Appendix, which is a part of this section, however, is valid for three-dimensional systems only if they are cubic. In that case the site Green's functions and self-energies are simply proportional to the 3×3 unit matrix.

In the CPA, a self-energy ansatz is made for the configuration-averaged Green's function,

$$\overline{\underline{G}} = \underline{P} + \underline{P}\,\underline{\Sigma}\,\overline{\underline{G}} \ , \tag{21}$$

where $\underline{\Sigma}$ is the self-energy. Because of the configuration average, $\overline{\underline{G}}$ has the translational symmetry of the perfect lattice and is therefore diagonal in a k representation. In the single-cell approximation (analogous to the *single-site* approximation for binary alloys) the k representation of $\underline{\Sigma}$ is independent of k, and in real space the large matrix $\underline{\Sigma}$ must be given by

$$\underline{\Sigma} = \sum_l \underline{\sigma}_l \ , \tag{22}$$

where $\underline{\sigma}_l$ is everywhere zero except possibly with-

in a $2n\times 2n$ block in the unit cell l. The $4n^2$ matrix elements of this block are independent of l. For convenience we write

$$\sigma_{\alpha\beta}\equiv (M_\alpha M_\beta)^{1/2}\tilde{\epsilon}_{\alpha\beta}x \quad . \tag{23}$$

Similarly, the single-cell t matrix $\underline{t}_l$ is possibly nonzero only in the $2n\times 2n$ block at cell l,

$$\underline{t}_l=(1-\underline{\overline{G}}_{ll}\underline{v}_l)^{-1}\underline{v}_l \ , \tag{24}$$

where $\underline{v}_l$ is given by

$$\begin{aligned}\underline{v}_l &\equiv M_1\underline{\epsilon}x-\underline{\sigma}_l=M_1\times(\underline{\epsilon}-\underline{\tilde{\epsilon}})\\ &\quad \text{if } l \text{ is a defective cell,}\\ &\equiv -\underline{\sigma}_l\\ &\quad \text{if } l \text{ is a host cell.}\end{aligned} \tag{25}$$

The single-cell t matrix approximately represents the scattering of phonons in a reference lattice, which is the configuration-averaged lattice. Self-consistency therefore requires that the configuration average of t_l vanish. In terms of the intracell Green's function,

$$F_{\alpha\beta}\equiv (M_\alpha M_\beta)^{1/2}\overline{G}_{ll\alpha\beta} \ , \tag{26}$$

the self-consistency condition becomes a $2n\times 2n$ matrix equation. Within any cell, dropping the index l, we have

$$\begin{aligned}&c[1+x(\underline{\tilde{\epsilon}}-\underline{\epsilon})\underline{F}]^{-1}(\underline{\tilde{\epsilon}}-\underline{\epsilon})\\ &\quad+(1-c)[1+x\underline{\tilde{\epsilon}}\,\underline{F}]^{-1}\underline{\tilde{\epsilon}}=0 \quad .\end{aligned} \tag{27}$$

We may rewrite Eq. (27) as

$$\underline{\tilde{\epsilon}}-c\underline{\epsilon}+x\underline{\tilde{\epsilon}}\,\underline{F}(\underline{\tilde{\epsilon}}-\underline{\epsilon})=0 \quad . \tag{28}$$

The above matrix equation yields $4n^2$ scalar equations, one for each element. In the Appendix we prove that for defects only on sublattice 1 only the (1, 1) element of $\underline{\tilde{\epsilon}}$ (and of $\underline{\sigma}$ and $\underline{\Sigma}$) is nonzero. The proof is valid for one-dimensional systems or square two-dimensional systems or cubic three-dimensional systems. Therefore the self-energy equation (21) takes on a particularly simple form. For the configuration-averaged Green's functions $\overline{G}_{\alpha\beta}(k)$ we find

$$\overline{G}_{11}(k)=\Delta(k)P_{11}(k) \ , \tag{29a}$$

$$\begin{aligned}\overline{G}_{22}(k)&=P_{22}(k)+P_{21}(k)\Sigma_{11}\\ &\quad\times\Delta(k)P_{12}(k) \ ,\end{aligned} \tag{29b}$$

$$\overline{G}_{12}(k)=\Delta(k)P_{12}(k) \ , \tag{29c}$$

$$\begin{aligned}\overline{G}_{21}(k)&=P_{21}(k)+P_{21}(k)\Sigma_{11}\\ &\quad\times\Delta(k)P_{11}(k) \ ,\end{aligned} \tag{29d}$$

$$\Delta(k)=[1-P_{11}(k)\Sigma_{11}]^{-1} \quad . \tag{30}$$

Because of the single-cell approximation, $\langle k|\hat{\Sigma}_{11}|k\rangle$ is not a function of k or k' but is only $\Sigma_{11}(x)$. However, because the defects are restricted to a single sublattice, the defects do mix the two branches of the phonon system and $\langle kj|\hat{\Sigma}|k'j'\rangle$ is not diagonal on j, j'. Also, because

$$\tilde{\epsilon}_{\alpha\beta}=\delta_{\alpha 1}\delta_{\beta 1}\tilde{\epsilon}_{11}\equiv\delta_{\alpha 1}\delta_{\beta 1}\tilde{\epsilon} \ , \tag{31}$$

the CPA equation becomes

$$x\tilde{\epsilon}_{11}F_{11}(\tilde{\epsilon}_{11}-\epsilon_{11})=(c\,\epsilon_{11}-\tilde{\epsilon}_{11}) \quad . \tag{32}$$

But from Eqs. (26) and (21)–(23),

$$\begin{aligned}F_{11}&=\frac{1}{N}\sum_k\{[M_1P_{11}(k)]^{-1}-x\tilde{\epsilon}_{11}\}^{-1}\\ &\equiv\frac{M_1}{N}\sum_k\overline{G}_{11}(k) \quad .\end{aligned} \tag{33}$$

We now specialize to one-dimensional systems. Using Eq. (11) for $P_{11}(k)$, we find after some algebra a solvable CPA equation [we drop subscripts (11) on ϵ_{11} and $\tilde{\epsilon}_{11}$ for convenience]:

$$\begin{aligned}&[x-X_T-\tilde{\epsilon}\,(x-X_2)][x-X_1-\tilde{\epsilon}x][c\epsilon-\tilde{\epsilon}]^2\\ &\quad=(\tilde{\epsilon}-\epsilon)^2\tilde{\epsilon}^2x(x-X_2) \ ,\end{aligned} \tag{34}$$

a cubic equation in $\tilde{\epsilon}$ to be solved numerically for the complex function $\tilde{\epsilon}(x)$.

Similarly we find an expression for a configuration-averaged Green's function in terms of the perfect-chain Green's function

$$\begin{aligned}\overline{G}_{ll\,11}(x)&=[(x-X_2)/(z-X_2)]\\ &\quad\times P_{ll\,11}(z) \ ,\end{aligned} \tag{35}$$

where

$$\begin{aligned}z&\equiv\tfrac{1}{2}X_T+[(x-\tfrac{1}{2}X_T)^2\\ &\quad-\tilde{\epsilon}\,x(x-X_2)]^{1/2} \quad .\end{aligned} \tag{36}$$

To find an analogous equation for $\overline{G}_{22}$ it is convenient to rewrite Eq. (29b) as

$$\begin{aligned}\overline{G}_{22}(k)&=P_{22}(k)+P_{21}(k)P_{11}^{-1}(k)\\ &\quad\times[\overline{G}_{11}(k)-P_{11}(k)]\\ &\quad\times P_{11}^{-1}(k)P_{12}(k) \quad .\end{aligned} \tag{37}$$

Using

$$\begin{aligned}P_{21}(k)P_{12}(k)&=\frac{\cos^2(\frac{1}{2}ka)}{M_1M_2}\\ &\quad\times\frac{X_AX_O}{[x-x_A(k)]^2[x-x_O(k)]^2}\end{aligned} \tag{38}$$

and

$$\cos^2(\tfrac{1}{2}ka)=1-x_A(k)x_O(k)/(X_AX_O) \ , \tag{39}$$

we finally find

$$\overline{G}_{ll22}(x)=P_{ll22}(x)+\frac{M_1}{M_2}\frac{1}{x-X_2}$$

$$\times (z - x_1) P_{ll\,11}(z)$$
$$- (x - X_1) P_{ll\,11}(x)] \quad . \tag{40}$$

The configuration-averaged Green's functions $\overline{G}_{ll11}(x)$ and $\overline{G}_{ll22}(x)$ are useful for calculating physical properties which depend directly on the diagonal element of the displacement-displacement correlation function. However, for this work we are primarily interested in the density of states and in the electric susceptibility.

C. Physical properties

The density of vibrational states for any system is given by

$$g(x) = \frac{1}{2\omega} g(\omega) = \frac{-1}{\pi N} \operatorname{Im} \operatorname{Tr} \langle MG \rangle_{av}$$
$$= \frac{-1}{\pi} \operatorname{Im} \sum_{\alpha} \langle M_{0\alpha} G_{00\alpha\alpha}(x) \rangle_{av} \quad , \tag{41}$$

where $G(x)$ is the retarded function, like $P(x)$ in Eq. (10). Also, $\langle \cdots \rangle_{av}$ means configuration average as does a bar over a single symbol. Therefore, we need to calculate conditional configuration-averaged Green's functions $\overline{G}^{d}_{00\alpha\alpha}$ and $\overline{G}^{h}_{00\alpha\alpha}$, where only those configurations with a defect (d) in the cell $l = 0$ are included in the averaging for $\overline{G}^{d}_{00\alpha\alpha}$, and only those configurations with a host atom (h) in the cell $l = 0$ are included in $\overline{G}^{h}_{00\alpha\alpha}$ $(= \overline{G} - \overline{G}^{d})$. Then

$$g(x) = -\frac{1}{\pi} \operatorname{Im}[M_2 \overline{G}_{00,22} + M_1 \overline{G}^{h}_{0011}$$
$$+ M_1' \overline{G}^{d}_{0011}]. \tag{42}$$

Because

$$\overline{G} = P + PC\overline{G}^{d} \quad , \tag{43}$$

using Eqs. (21)–(23) we find an expression similar to Taylor's,[14]

$$g(x) = -\frac{1}{\pi} \operatorname{Im}[M_2 \overline{G}_{0022}$$
$$+ M_1 (1 - \tilde{\epsilon}_{11}) \overline{G}_{0011}] \quad . \tag{44}$$

This expression, in terms of the unconditional configuration averages and the self-energy, is used to calculate the density of states in Sec. IV.

We also wish to calculate the dielectric susceptibility,

$$\chi(x) \equiv \chi(k = 0, \omega^2) \quad ,$$
$$\chi(x) = (N)^{-2}$$
$$\times \sum_{ll'\alpha\beta} \langle Q_{l\alpha} Q_{l'\beta} G_{ll'\alpha\beta}(x) \rangle_{av} \quad , \tag{45}$$

where $Q_{l\alpha}$ is the charge, or the Szigeti effective charge, on the ion at (l, α). Since effective charges may differ for host and defect atoms, a proper calculation of χ requires the calculation of configuration averages which are conditional on both the first and second sites of the Green's function $\overline{G}^{ij}$, where i and j take on the values h and d for host and defect atoms on sublattice 1. Then, in terms of the Fourier-transformed conditionally averaged Green's functions $\overline{G}^{ij}_{\alpha\beta}(\vec{k})$,

$$\chi = Q_2^2 \overline{G}_{22}(0) + \sum_{i=h,d} Q_2 Q_i$$
$$\times [\overline{G}^{i}_{21}(0) + \overline{G}^{i}_{12}(0)]$$
$$+ \sum_{ij=h,d} Q_i Q_j \overline{G}^{ij}_{11}(0) \quad . \tag{46}$$

The calculation of χ is considerably simplified if both host and defect ions have the same charge. In that case the ionic charge is associated unambiguously with the sublattice and only unconditional configuration-averaged Green's functions are needed to find

$$\chi(x) = \sum_{\alpha\beta} Q_\alpha Q_\beta \overline{G}_{\alpha\beta}(k = 0, x) \quad . \tag{47}$$

Because the Green's functions in Eq. (46) are evaluated at $k = 0$ it is a simple matter to use Eqs. (29) and (12) to calculate the real and imaginary parts of the susceptibility. For the special case of point-charge ions and charge neutrality,

$$Q_1' = Q_1 = -Q_2 \quad , \tag{48}$$

we find

$$\chi(x) = \frac{Q_1^2}{M_1} \frac{1 + \beta[1 - \tilde{\epsilon}(x)]}{x - X_T - (x - X_2)\tilde{\epsilon}(x)} \quad . \tag{49}$$

In the limit $c = 0$ or $\tilde{\epsilon} = 0$ and in the limit $c = 1$, where $\tilde{\epsilon} = \epsilon$, this expression reduces to the perfect-chain susceptibility.

IV. NUMERICAL RESULTS

A. Density of states

In Figs. 3 and 4 we compare the CPA density of states with the spectra computed numerically by Painter[15] for 20 000-atom chains. These computer experiments are of the type introduced by Dean.[16] Although an averaged Green's-function method cannot reproduce all the detailed features of the computer experiment, the over-all agreement is quite good. In Fig. 3, $\beta = 0.5$, $\epsilon = 0.5$, $c = 0.5$, substitution is made on the light sublattice by still lighter atoms. The five band-edge positions are given exactly by the CPA and the strengths of all three bands are also reproduced quite well. This density of states may be roughly understood as the approximate superposition of spectra for two ordered diatomic chains, the first with masses $M_1 = 2$, $M_2 = 4$, so that $X_A = 0.5$, $X_O = 1$, $X_T = 1.5$, and the second with masses $M_1' = 1$, $M_2 = 4$ so that $X_A = 0.5$, $X_O = 2$, $X_T = 2.5$. The suc-

cess of the CPA can be understood by considering the localization in space of the eigenstates of the disordered system.[17] At low frequencies, where the CPA calculation coincides almost perfectly with the computer experiment, the eigenstates are extended, the true density of states is insensitive to the details of the chain structure, and the CPA mean-field calculation then is very good. Moreover for this case, where the bands are relatively narrow compared to their separation, the eigenstates in the two optic bands of the disordered system are rather localized in space. Therefore, the single-cell approximation, which neglects correlation between scatterings in different unit cells becomes valid. Not surprisingly, the CPA spectrum agrees better with the upper optic experimental band, where the states are most localized, than with the lower optic band. Our viewpoint here is similar to that of Ref. 8, where it is shown that the CPA for electrons is exact in the atomic limit. Narrow bands of lattice vibrations, the "Einstein limit," occur in the limit $M_2=\infty$. It is not difficult to show that in this limit the CPA for the vibrational density of states is exact. The self-energy can be evaluated in closed form,

$$\tilde{\epsilon}(x)=c\epsilon(X_T-x)/[X_T-x+\epsilon x(1-c)]\ ,$$

and

$$g(x)=\delta(x)+(1-c)\delta(x-X_T)$$
$$+c\,\delta[x-X_T/(1-\epsilon)]\ .$$

In Fig. 4, $\beta=\frac{1}{3}$, $\epsilon=0.5$, $c=0.5$, light defects are substituted onto the heavy sublattice. The spectrum is not well approximated by the overlap of ordered diatomic spectra of chains with $M_1=2$, $M_2=1.5$, so that $X_A=1$, $X_O=\frac{4}{3}$, $X_T=\frac{7}{3}$, and with $M_1'=1$, $M_2=1.5$, so that $X_A=\frac{4}{3}$, $X_O=2$, $X_T=\frac{10}{3}$, though remnants of the band-edge singularities can be seen in the spectrum. The large amount of structure in the upper part of the experimental band can be attributed to the vibrations of complexes of atoms, triples, four-atom clusters and the like. Although such details can be reproduced by a cluster CPA,[15,17] the single-cell CPA used here provides only a rough guide to the regions of appreciable spectral weight.

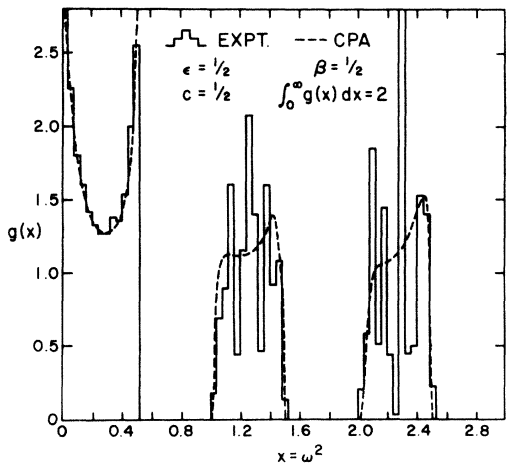

FIG. 3. Density of states for the mixed diatomic chain with $\beta\equiv M_1/M_2=0.5$, $\epsilon\equiv 1-M_1'/M_1=0.5$, and $c\equiv$ (concentration of defects) $=0.5$. The histogram shows the results of Painter's computer experiment for a 20 000 atom chain. The dotted curve shows the prediction of the single-cell CPA.

B. Optical properties of mixed diatomic systems

As suggested in Sec. I, we are principally interested in the CPA solution of the mixed diatomic chain as a means to determine the nature of the reflectivity bands of real mixed diatomic systems. We find here that our theory can provide a satisfactory explanation of one-mode–two-mode behavior. However, the application of our one-dimensional theory to three-dimensional systems requires some qualification and some explanation.

The reflectivity of real systems is given by $R=|(n-1)/(n+1)|^2$, where n is the complex refractive index, $n=\epsilon^{1/2}$. The complex dielectric constant is given by $\epsilon=1+4\pi\chi$, where χ is the electric susceptibility. We do not calculate the reflectivity with our one-dimensional model. However, we note that for real systems the peaks in R are associated with peaks in $\mathrm{Im}\chi$.[18] At such a peak the real part of χ becomes negative and R becomes large. In fact, the configuration-averaged long-wavelength susceptibility of a disordered system is mathematically of the damped form indicated by Burstein,[18] and Burstein's picture may be applied literally to this case. Therefore we argue that the reflectivity of a real system should have one or two peaks if $\mathrm{Im}\chi$ has one or two peaks, though the peak in reflectivity occurs at somewhat higher frequencies than the peak in $\mathrm{Im}\chi$. In cases of doubt, $\mathrm{Re}\chi$ can be examined for the number of sign changes.

Our next step is to argue that the variation of χ for a real system can be reliably determined from a one-dimensional model. Because the photon-lattice interaction is proportional to the dot product between photon polarization and atomic displacement vectors, light sees only one component of atomic displacements, namely, a $k=0$ transverse component. We are quite free to interpret the displacements $u_{l\alpha}$ in the equation of motion, Eq. (2), as transverse displacements. The assumptions of our model for the electrodynamics of polar crystals are not optimum; in particular no allowance is made for the fact that different pure

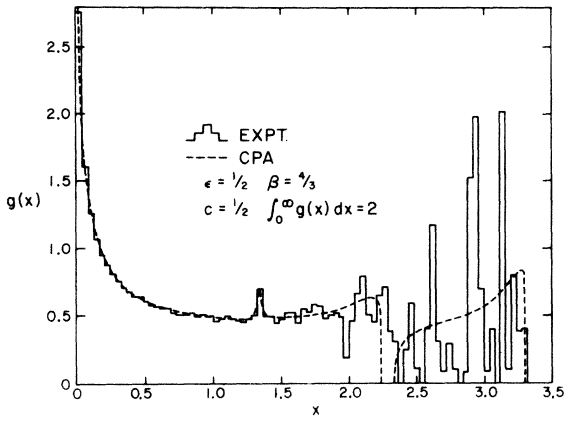

FIG. 4. Density of states for the mixed diatomic chain with $\beta \equiv M_1/M_2 = \frac{4}{3}$, $\epsilon \equiv 1 - M_1'/M_1 = 0.5$, and $c \equiv$ (concentration of defects) $= 0.5$. The histogram shows the results of Painter's computer experiment for a 20 000-atom chain. The dotted curve shows the prediction of the single-cell CPA.

materials will have different values of $\epsilon_0/\epsilon_\infty$ and therefore different reflectivity bandwidths.[19] Furthermore, we do not use the appropriate Szigeti effective charge to allow for differing polarizabilities of the various atomic species, but instead we consistently assume point charges and charge neutrality, Eq. (48). Still further, our model does not consider the change in force constants between atoms, though the experimental reflectivity bands of the ordered end members frequently reveal that force-constant changes do occur and should be included in a complete theory for the intermediate-mixed systems. Nor do we consider anharmonic broadening of the optically active modes.

The advantage gained by these assumptions is that we are able to identify unambiguously the results of treating the disorder among the atomic masses by the CPA. Since the mass disorder appears to be the most important single feature of these mixed diatomic systems we expect our theory to agree with experiment over all.

There is another difficulty in applying our one-dimensional theory to three-dimensional systems. Although the mathematical form of the one-dimensional $\bar{G}(k=0)$ is adequate to represent the three-dimensional system, the resonant denominator Δ in Eq. (30) is not a good approximation to the corresponding three-dimensional quantity. The effect of the one-dimensional resonance can be seen in the low-concentration limit or in the single-defect problem. The graphs of P_{ll} in Fig. 2 show that a solution of the resonance equation, Eq. (20), exists for all $\epsilon > 0$. By contrast, in three dimensions the parameter ϵ must exceed a critical positive value ϵ_c in order for a local mode to form. As the concentration of defects is increased, the tendency then is for the one-dimensional model to produce a spurious band associated with a broadened local mode. We can identify such behavior by the method introduced by Lucovsky *et al.*[4] These authors proposed that a real three-dimensional system could be mimicked by a one-dimensional chain by redefining the zone-boundary frequencies in terms of the experimental longitudinal- and transverse-optic-mode frequencies, X_{LO} and X_{TO},

$$3X_1 + 3X_2 = 2X_{\mathrm{TO}} + X_{\mathrm{LO}} \ , \tag{50a}$$

and

$$X_2/X_1 = M_1/M_2 \equiv \beta \ . \tag{50b}$$

Requiring that a local mode lie above X_{LO} leads to a critical-mass-change parameter

$$\epsilon_c = [\tfrac{2}{3}(1-\gamma)]^{1/2}\left(\frac{2+3\beta-2\gamma}{3+2\beta-2\gamma\beta}\right)^{1/2} \ , \tag{51}$$

where $\gamma = X_{\mathrm{TO}}/X_{\mathrm{LO}}$ ($= \epsilon_\infty/\epsilon_0$ for cubic systems). If $\epsilon > \epsilon_c$ then Lucovsky, Brodsky, and Burstein (LBB) expect that a local mode will form for small concentrations of a light defect and that the corresponding mixed crystal will show two-mode behavior.

To compensate for the spurious local modes of the one-dimensional model we supplement our CPA calculations with the criterion of LBB. We expect that our model will fail when $\epsilon > \epsilon_c$; we expect our model to hold good when $\epsilon > \epsilon_c$. It will be seen that this procedure *does not* always lead to a prediction of two-mode behavior. Because $\epsilon_c = 0$ for $\gamma = 1$, our model is more successful for III-V and II-VI systems for which $\epsilon_\infty \approx \epsilon_0$, than it is for I-VII systems, for which γ tends to be small.

In the following paragraphs we compare the CPA theory for the dielectric susceptibility with the results of optical experiments on five selected mixed III-V, II-VI, and I-VII crystals. We also note the one-mode–two-mode predictions of several recent theories based on the low-cencentration limit. The simplest such theory is the MREI model of Chang and Mitra.[3] A second criterion, which includes a measure of the polarizabilities of the constituents, predicts that a system will show two-mode behavior when the method of LBB[4] predicts a local mode for small c. A third criterion, which also includes atomic polarizabilities, is that of Harada and Narita (HN).[19]

The mixed systems which we have chosen to discuss are ones for which recent experimental data is available. They are also systems which are controversial, for which the various criteria noted above disagree with one another or with experiment.

$In_{1-c}Ga_cSb$ ($\beta = 0.94$, $\epsilon = 0.39$, $\epsilon_c = 0.26$). The experimental reflectivity reported by Brodsky *et al.*[5] is shown in Fig. 5. The MREI model predicts one-mode behavior, but the criterion of LBB predicts two-mode behavior. Brodsky *et al.* claim that, as in the case of $In_{1-c}Ga_cAs$, the experimental results do not fall into either category, but they call the system "two-mode" for $c > 0.7$. The concentration of In must be increased to $(1-c) = 0.3$ before there is any experimental indication of a second peak. Moreover, the frequency of the upper peak changes considerably with concentration. Comparison with the CPA theory shows that the theory is able to account for the anomalous behavior observed. The lower peak appears when $c = 0.7$ in the experiment and when $c = 0.6$ in the CPA theory. At all concentrations the relative strengths of the bands are given fairly well by the theory. The goodness of agreement between theory and experiment is disguised by the fact that there is a 14% force-constant decrease proceeding from GaSb to InSb, which is not taken into account in the theory for diagonal disorder. If this effect is included by a simple virtual crystal calculation then the frequencies of experimental and theoretical peaks nearly coincide. As c is decreased from 0.6 to 0.05, the lower theoretical peak moves up significantly to higher frequencies and the upper theoretical peak moves down considerably, in agreement with the observed behavior of the reflectivity. Without force-constant changes the upper peak frequency is shifted by about 5% over the concentration range.

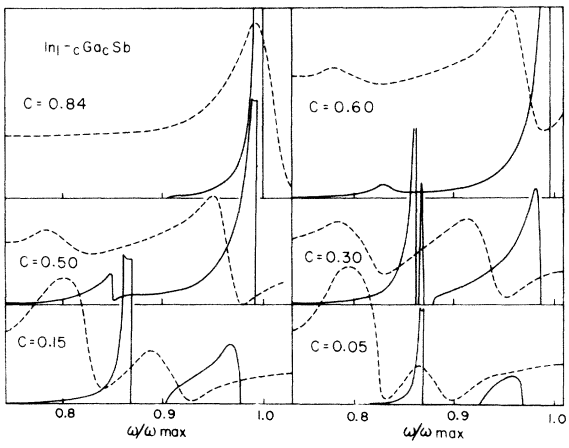

FIG. 5. (---) experimental reflectivity of $In_{1-c}Ga_cSb$ reported in Ref. 5. (—) CPA theory for Imχ. The calculated frequencies are scaled to the experimental peak at $c = 1.0$ and therefore Imχ is shifted to higher frequencies. The absolute scale of the experimental reflectivity is arbitrary as is the zero of reflectivity, but the relative scale between theory and experiment is the *same* for all six concentrations.

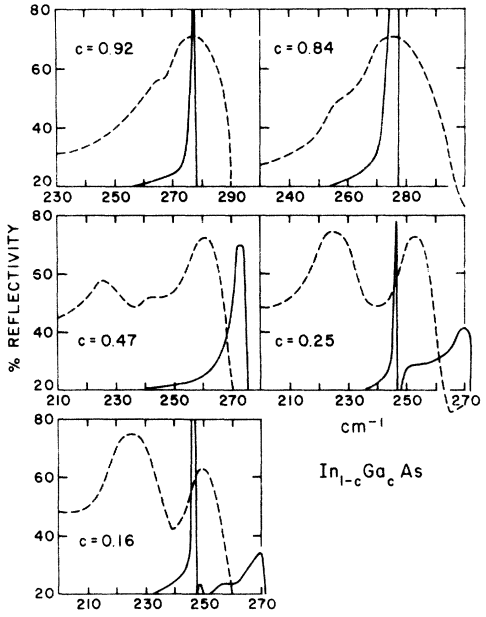

FIG. 6. (---) experimental reflectivity of $In_{1-c}Ga_cAs$ reported in Ref. 2. (—) CPA theory for Imχ. The calculated frequencies are scaled to the experimental peak at $c = 1.0$ and therefore Imχ is shifted to higher frequencies. The absolute scale of Imχ is arbitrary but the relative scale between theory and experiment is the *same* for all five concentrations. The ordinate values are those of the experiment and the zero has been suppressed. The value of Imχ on the horizontal axis, however, is zero.

$In_{1-c}Ga_cAs$ ($\beta = 1.53$, $\epsilon = 0.39$, $\epsilon_c = 0.43$). The experimental reflectivity reported by Lucovsky and Chen[2] is shown in Fig. 6. The MREI and the criterion of LBB both predict one-mode behavior. Lucovsky and Chen note that, as in the case of $In_{1-c}Ga_cSb$, $GaSb_{1-c}As_c$, and $InSb_{1-c}As_c$, the experimental results do not fall into either category, but they call the system "two-mode" for $c < 0.8$. The experimental behavior observed is very similar to that for $In_{1-c}Ga_cSb$. Comparison with the CPA theory shows that the theory is able to account for the anomalous behavior observed. The lower peak appears when $c \approx 0.5$ in the experiment and for somewhat smaller c in the theory. For c as low as 0.25 the CPA theory produces two distinct peaks separated by a small region where Im$\chi = 0$. At $c = 0.25$ and 0.16 the relative strengths of the two peaks are given fairly well by the theory. The goodness of agreement between theory and experiment is obscured by the fact that there is a 18.5% force-constant decrease on going from GaAs to InAs which is not included in the theory. If this effect is included by a virtual-crystal calculation then the frequencies of the experimental and theoretical peaks nearly coincide as shown in Table I.

TABLE I. Comparison of the frequencies of the peaks in Imχ from Fig. 6 for $In_{1-c}Ga_cAs$, as calculated by the CPA theory, and the CPA adjusted by a 18.5% force-constant change in a virtual-crystal sense, with the frequencies of the experimental peaks observed in the reflectivity.

	Upper peak			Lower peak		
c	CPA	CPA(adj)	Expt.	CPA	CPA(adj)	Expt.
0.84	277	273	275			
0.47	273	260	260	···	···	225
0.25	270	251	253	246	228	225
0.16	269	248	250	246	226	225

$Cd_{1-c}Zn_cTe$ ($\beta = 0.87$, $\epsilon = 0.42$, $\epsilon_c = 0.45$). The experimental reflectivity reported by HN[19] is shown in Fig. 7. The MREI model and the criterion of LBB predict that the system should be one-mode but the criterion of HN predicts two-mode behavior. Harada and Narita claim that the experimental results show two-mode behavior. According to the criterion of LBB, the local mode predicted by the one-dimensional model at 170 cm^{-1} should be discarded. If we retain it we find that the CPA theory gives a good qualitative account of the experimental results. Experimentally the upper peak frequency increases somewhat as c is increased, while the lower peak frequency remains constant. The CPA theory reproduces the shift of the upper peak but also predicts that the lower peak should decrease significantly as c increases, contrary to experiment. In contrast to the comparison between theory and experiment for III-V systems the discrepancies in peak positions cannot be understood by a simple force-constant change.

$Cd_{1-c}Zn_cS$ ($\beta = 3.5$, $\epsilon = 0.42$, $\epsilon_c = 0.7$). The experimental reflectivity reported by Lisitsa *et al.*[20] is shown in Fig. 8. The MREI model, and the criteria of LBB and HN all agree that the system should show one-mode behavior. It is claimed that the experiments of Lisitsa *et al.* show one-mode behavior, though only two mixed crystals, both near 50-50 composition, were studied. The CPA theory supports the contention that this system is one-mode. The distinct local mode does not appear in the one-dimensional CPA theory except at rather small concentrations. Because ϵ_c is very much larger than ϵ, this local mode can be discarded as unphysical. The discrepancy between theory and experiment in relative peak heights for $c = 0.35$ and $c = 0.45$ might be attributed to the unphysical local mode in the one-dimensional theory. Furthermore, the reflectivities of the end members suggest a rather enormous force-constant change, a decrease of 25% on going from ZnS to CdS, which is not included in the theory.

$Rb_{1-c}K_cI$ ($\beta = 1.07$, $\epsilon = 0.55$, $\epsilon_c = 0.5$). The imaginary part of the dielectric constant, determined by a Kramers-Kronig analysis of a multiple-oscillator fit to the experimental reflectivity reported by Fertel and Perry,[21] is shown in Fig. 9. The MREI model, and the criteria of LBB and of HN all agree that the system should exhibit two-mode behavior. Fertel and Perry claim that the experimental results show two-mode behavior. This claim appears to be the only uncontested claim for two-mode behavior in an alkali halide, although the MREI model and the criterion of LBB predict that $Rb_{1-c}K_cBr$, $RbBr_{1-c}Cl_c$ and $Rb_{1-c}Na_cI$ should also be two-mode. The CPA theory supports the contention that the system should exhibit two-mode behavior. At all large values of c the theory produces two well-separated peaks in Imχ. The upper peak is associated with the local mode at small values of c, which we retain as physical since $\epsilon > \epsilon_c$. The local mode is broadened and shifted to higher frequencies as c is increased. This behavior agrees with experiment though the experimental shift is about 7% and the theoretical shift is 5%. Recently Taylor[10] has performed a three-dimensional CPA calculation for this system. His results also indicate two-mode behavior.

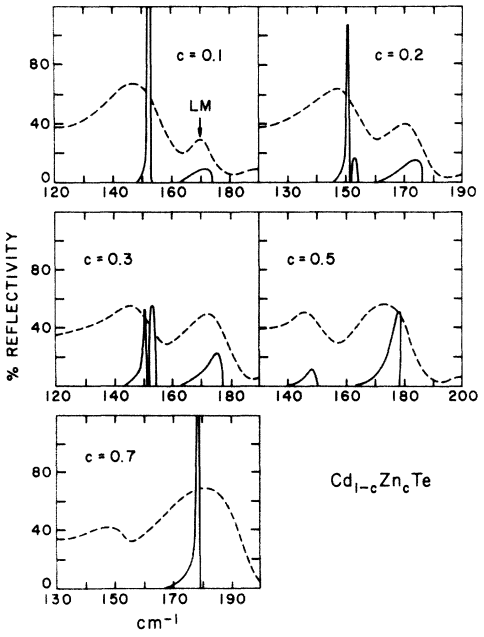

FIG. 7. (---) experimental reflectivity of $Cd_{1-c}Zn_cTe$ reported in Ref. 19. All ordinate scales are the same. (—) CPA theory for Imχ. The calculated frequencies are scaled to the experimental peak at $c = 1.0$ and therefore Imχ is shifted to higher frequencies. The absolute ordinate scale for Imχ is arbitrary but the relative scale between theory and experiment is the *same* for all five concentrations.

V. DISCUSSION

In this paper we have generalized the CPA for the lattice dynamics of mass disordered systems to the case of mixed diatomic systems. Specific results were obtained in the case of one dimension. We compared the CPA configuration-averaged density of states for several infinitely long mixed chains with the density of states determined by computer experiments on long chains. We also compared the CPA dielectric susceptibility with the reflectivity and dielectric constant of mixed polar crystals. We believe that the CPA and the one-dimensional model can account for the experimentally observed optical properties of these systems over the entire concentration range. However, in order to obtain improved agreement between theory and experiment several other factors should be taken into account. These factors include force-constant changes, anharmonic line broadening, and atomic polarizability. Furthermore, some means, such as the criterion of Lucovsky *et al.*,[4] must be used to eliminate unphysical local modes sometimes produced by the one-dimensional model. Although the comparison of theory with experiment is complicated by these effects, we find that the CPA calculation can at least account for the one- or two-mode nature of mixed diatomic systems and for variations on one- and two-mode behavior. However, this traditional classification depends on a more or less subjective interpretation of the experimental results. A theory which can predict a complete spectrum at any composition for comparison with the observed spectrum is obviously more satisfactory. Especially for those III-V systems which appear to switch from one-mode to two-mode behavior, the advantage of the CPA theory over all previous theories should be clear. Because the CPA can interpolate between single and split-band behavior as a function of concentration and scattering strength it is uniquely sucessful for these systems. It seemed worthwhile to study this effect in more detail.

We wish to study the nature of the optic vibrational bands predicted by the single-cell CPA for one-dimensional mixed diatomic systems. Because of the complications involved in predicting reliable optical behavior we consider instead the density of states in the optic bands which is closely re-

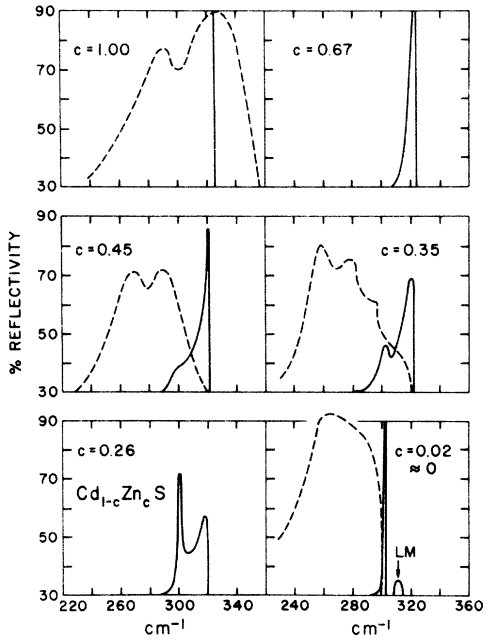

FIG. 8. (---) experimental reflectivity of $Cd_{1-c}Zn_cS$ reported in Ref. 20; (—) CPA theory for Imχ. The calculated frequencies are scaled to the experimental peak at $c = 1.0$ and therefore Imχ is shifted to higher frequencies. The absolute ordinate scale for Imχ is arbitrary but is the same for all six concentrations. The ordinate values are for the experimental reflectivity, the same for all four concentrations, and the zero is suppressed. However, on the horizontal axis, Imχ is zero. The lower right-hand figure includes the experiment for $c = 0$ and the theory for $c = 0.02$, showing the broadened local mode (LM).

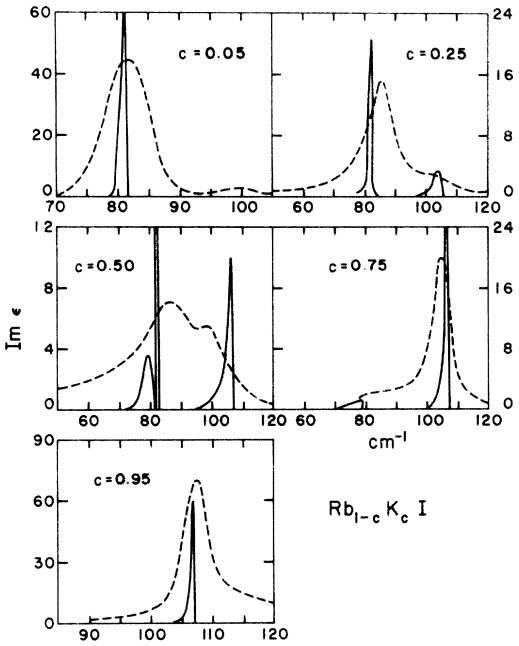

FIG. 9. (---) imaginary part of the dielectric constant of $Rb_{1-c}K_cI$ determined by Kramers-Kronig analysis of experiment in Ref. 21; (—) CPA theory for Imχ. The calculated frequencies are scaled to the experimental peak at $c = 1.0$. The absolute scale of Imχ is arbitrary, but the relative scale between theory and experiment is the *same* for all five concentrations. The ordinate values are those of the experiment.

lated to the imaginary part of the susceptibility. We define a "two-band" system as one with a gap in the density of states at optic-mode frequencies. A "one-band" system is one in which there is no gap in the density of states, apart from a possible gap between acoustic and optic modes. Because rapid variations, singularities, or damped singularities in $\mathrm{Re}\chi$ occur at frequencies near the peaks in $\mathrm{Im}\chi$ negative values of the real part of the dielectric function occur near peaks in the density of states. Therefore systems which are strongly one- or two-band are expected to be one- or two-mode, respectively. The distinction between the behavior of the density of states and that of the optical properties becomes important only near transitions from one to two-band behavior.

A phase diagram for three intermediate concentrations is shown in Fig. 10. Above the phase boundary, one-band behavior occurs; below this line two-band behavior occurs. As the concentration c of the light constituent is reduced, the phase boundary rises towards the low-concentration limit, in which one-band behavior never occurs because of the necessary presence of local modes. We find that for small concentrations and large ϵ the phase boundary becomes a broad one. The error bar for $c = 0.25$ and $\epsilon = 0.5$ includes values of β all of which satisfy our criterion for the onset of a gap in the density of states. The four mixed systems which Lucovsky and Chen[2] have claimed to change from one to two mode as c is decreased all have $\epsilon \lesssim 0.4$ and fall between the phase boundaries for $c = 0.5$ and $c = 0.2$.

We have included the Chang-Mitra (MREI) criterion for one- or two-mode behavior, $\beta = \epsilon/(1-\epsilon)$, on Fig. 10. It is easy to see why the CPA phase

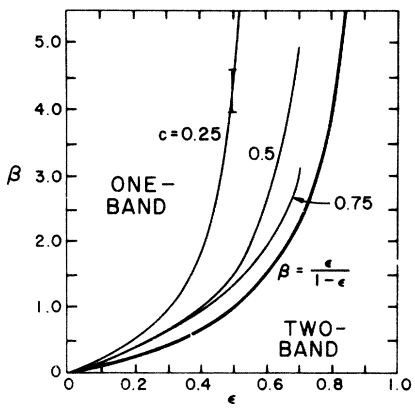

FIG. 10. CPA phase boundary between mixed diatomic systems $AB_{1-c}C_c$ with one optic band and two optic bands in the density of states for three concentrations of the light constituent. $\beta \equiv M_1/M_2 \equiv M_B/M_A$, $\epsilon \equiv 1 - M_1'/M_1 \equiv 1 - M_C/M_B$. The MREI criterion is the curve on the right-hand side.

boundaries for all concentrations lie above the MREI curve by starting with a two-crystal model for $AB_{1-c}C_c$. In terms of our former notation, $M_A = M_2$, $M_B = M_1$, $M_C = M_1'$. Since $M_B > M_C$, the top of the optic band in AB will always be lower in frequency than the top of the optic band in AC. For $M_A < M_C < M_B$ the optic bands must overlap. For $M_A > M_C$, and $M_A \lesssim M_B$, the top of the optic band in AB occurs at $2f/(1/M_A + 1/M_B)^{-1}$ and the bottom of the optic band in AC occurs at $2f/M_C$ for equal force constants. The MREI condition for two-mode behavior, $M_C^{-1} > (1/M_A + 1/M_B)$, is then simply the requirement that the optic modes of AB and AC not overlap. This requirement is plausible since the Saxon-Hutner hypothesis insists that the mixed system cannot have modes at frequencies outside the bands of AB and AC. However, the CPA bands also satisfy the Saxon-Hutner hypothesis; the CPA bands are usually narrower than the bands allowed by the theorem for the mixed system. Therefore two bands calculated in the CPA do not overlap as readily as the independent crystal model would suggest. We expect, therefore, that the MREI model would tend to predict one-mode behavior for systems which are actually two mode. Inspection of a number of individual cases reveals that this is the case.

To illustrate the use of our phase diagram we compare theory and experiment for nine more mixed crystals.

$Rb_{1-c}K_cCl$ ($\beta = 2.41$, $\epsilon = 0.54$, $\epsilon_c = 0.5$). The reflectivity has been measured[22] at $c = 0.25$, 0.5, and 0.75. At $c = 0.25$ and 0.5 the experiments show two peaks; at $c = 0.75$ there is only 1 peak. Since ϵ and β place this system between the $c = 0.5$ and $c = 0.75$ phase boundaries, the CPA theory predicts the behavior observed experimentally.

$KBr_{1-c}Cl_c$ ($\beta = 2.05$, $\epsilon = 0.56$, $\epsilon_c = 0.7$). Fertel and Perry[21] find one-mode behavior throughout the concentration range. ϵ and β suggest that this system should be two-mode for $c < 0.5$, but since $\epsilon \ll \epsilon_c$ we must reject this prediction and expect one-mode behavior for all c.

$CdSe_{1-c}S_c$ ($\beta = 0.7$, $\epsilon = 0.59$, $\epsilon_c = 0.45$). The reflectivity measured by Verleur and Barker[23] shows two-mode behavior for $c = 0.015$, 0.27, 0.54, and 0.77. Since ϵ and β place this system firmly in the two-mode region for all c, the CPA agrees with experiment. Specific calculations show that the theory accounts well for the movements of the peak positions with c.

$ZnSe_{1-c}S_c$ ($\beta = 1.2$, $\epsilon = 0.59$, $\epsilon_c = 0.47$). The reflectivity reported by Chang and Mitra[1] shows two-mode behavior for $c = 0.015$, 0.33, 0.6, and 0.82. The above remarks comparing theory and experiment for $CdSe_{1-c}S_c$ apply to this system as well.

$GaSb_{1-c}As_c$ ($\beta = 1.74$, $\epsilon = 0.38$, $\epsilon_c = 0.3$). The reflectivity measured by Lucovsky and Chen[2] shows

two peaks at $c = 0.07$ and 0.11 and one peak at $c = 0.91$ and 0.93. Since ϵ and β place this system just above the $c = 0.25$ phase boundary, independent CPA runs were made. The theory is found to agree with the observed behavior of the reflectivity.

$InSb_{1-c}As_c$ ($\beta = 1.06$, $\epsilon = 0.38$, $\epsilon_c = 0.29$). The reflectivity[2] shows two peaks for $c = 0.2$ and 0.25 but one peak for $c = 0.85$. Since ϵ and β place this system between the $c = 0.25$ and $c = 0.5$ phase boundaries, the CPA theory agrees with experiment.

$GaAs_{1-c}P_c$ ($\beta = 1.09$, $\epsilon = 0.59$, $\epsilon_c = 0.33$). The reflectivity measured by Verleur and Barker[24] shows two-mode behavior for $c = 0.06$, 0.28, 0.56, 0.85, and 0.99. The above remarks comparing theory and experiment for $CdSe_{1-c}S_c$ apply to this system as well.

$InAs_{1-c}P_c$ ($\beta = 0.65$, $\epsilon = 0.59$, $\epsilon_c = 0.3$). The reflectivity reported by Chang and Mitra[1] shows two-mode behavior for all c. Since ϵ and β place this system firmly in the two-mode region the CPA theory agrees with experiment.

$Ga_{1-c}Al_cAs$ ($\beta = 0.93$, $\epsilon = 0.61$, $\epsilon_c = 0.31$). The reflectivity reported by Ilegems and Pearson[25] shows two-mode behavior for all c. Since ϵ and β place this system firmly in the two-mode region the CPA theory agrees with experiment.

ACKNOWLEDGMENTS

The authors are grateful to Dr. R. D. Painter for performing the computer experiment reported in Sec. IV A and to Dr. D. W. Taylor and Dr. G. Lucovsky for interesting correspondence. They also wish to thank Professor M. H. Cohen for useful discussions.

APPENDIX

We shall prove that for a mixed diatomic chain, in which the defects are only on sublattice number 1, the CPA self-energy $\underline{\tilde{\epsilon}}$ is zero except for $\tilde{\epsilon}_{11}$. Then clearly only the (1, 1) elements of $\underline{\sigma}$ and of $\underline{\Sigma}$ will be nonzero. Equation (28) of the text leads to four equations for the four matrix elements. We shall label these equations (α, β). For example, Eq. (1, 2) is

$$(\tilde{\epsilon}_{11}xF + \tilde{\epsilon}_{12}xF_{21} + \tilde{\epsilon}_{22}xF_{22} + 1)\,\tilde{\epsilon}_{12} = -\,\tilde{\epsilon}_{11}xF_{12}\tilde{\epsilon}_{22} \qquad (1,2)$$

Proof. Rearranging Eq. (28) and taking the determinant of both sides, we find

$$c \det \underline{\epsilon} = 0 = \det \underline{\tilde{\epsilon}} \times \det [\underline{1} + x\underline{F}(\underline{\tilde{\epsilon}} - \underline{\epsilon})] \ , \qquad (A1)$$

because only the (1, 1) element of $\underline{\epsilon}$ is nonzero.

In the limit of no defect, $\epsilon_{11} = 0$, we must have $\underline{\tilde{\epsilon}} = 0$ to regain the perfect-chain Green's function. In that case the last factor on the right-hand side of Eq. (A1) equals 1. Since we require continuity of our functions for small defect strength that factor cannot be zero as ϵ_{11} becomes finite. Therefore to satisfy Eq. (A1), $\det \underline{\tilde{\epsilon}} = 0$ or

$$\tilde{\epsilon}_{11}\tilde{\epsilon}_{22} = \tilde{\epsilon}_{12}\tilde{\epsilon}_{21} \ . \qquad (A2)$$

Substituting Eq. (A2) into the right-hand side of Eq. (1, 2), we find

$$[x\mathrm{Tr}(\underline{\tilde{\epsilon}}\underline{F}) + 1]\tilde{\epsilon}_{12} = 0 \ . \qquad (A3)$$

Let us first assume $\tilde{\epsilon}_{12} \neq 0$. From Eq. (28),

$$x\tilde{\epsilon}F = (c\underline{\epsilon} - \underline{\tilde{\epsilon}})\,(\underline{\tilde{\epsilon}} - \underline{\epsilon})^{-1} \qquad (A4)$$

The inverse above exists if $\tilde{\epsilon}_{22} \neq 0$. However, if $\tilde{\epsilon}_{22} = 0$, then either $\tilde{\epsilon}_{12} = 0$ (contrary to hypothesis) or else $\tilde{\epsilon}_{21} = 0$. But if $\tilde{\epsilon}_{21} = \tilde{\epsilon}_{22} = 0$, $\tilde{\epsilon}_{12} \neq 0$ from Eq. (1, 2) and from Eq. (1, 1) we find $c = 1$, which is not generally true. We conclude, therefore, that for $\tilde{\epsilon}_{12} \neq 0$ we have $\tilde{\epsilon}_{22} \neq 0$ and the inverse in Eq. (A4) exists, except, perhaps, at isolated points which are unimportant for our proof. But in order to satisfy Eq. (A3) the trace of Eq. (A4) must equal -1. Using Eq. (A2) we are able to simplify the expression on the right-hand side of Eq. (A4) to show that if $\tilde{\epsilon}_{12} \neq 0$ then Eq. (A3) is satisfied only if $c = 0$, which is not generally true. We conclude therefore that $\tilde{\epsilon}_{12} = 0$.

But if $\tilde{\epsilon}_{12} = 0$, then from Eq. (A3) either $\tilde{\epsilon}_{11} = 0$ or $\tilde{\epsilon}_{22} = 0$. If $\tilde{\epsilon}_{11} = \tilde{\epsilon}_{12} = 0$ then from Eq. (1, 1) we find $c\epsilon_{11} = 0$, which is not generally true. We conclude therefore that $\tilde{\epsilon}_{11} \neq 0$ and $\tilde{\epsilon}_{22} = 0$.

Let us suppose that $\tilde{\epsilon}_{12} = \tilde{\epsilon}_{22} = 0$, $\tilde{\epsilon}_{21} \neq 0$. Then from Eq. (2, 1),

$$x(\epsilon_{11} - \tilde{\epsilon}_{11})\,F_{11} = 1 + x\tilde{\epsilon}_{21}F_{12} \ ; \qquad (A5)$$

substituting from Eq. (1, 1) for the left-hand side of Eq. (A5), we find $c\epsilon_{11} = 0$, which is not generally true. Finally, therefore, we conclude,

$$\tilde{\epsilon}_{12} = \tilde{\epsilon}_{21} = \tilde{\epsilon}_{22} = 0, \quad \tilde{\epsilon}_{11} \neq 0$$

which completes the proof.

---

*Work supported by the National Science Foundation Grant No. GH34565.

†Present address: Xerox Research Center, Palo Alto, Calif. 94304.

[1] I. F. Chang and S. S. Mitra, Adv. Phys. 20, 359 (1971).

[2] G. Lucovsky and M. F. Chen, Solid State Commun. 8, 1397 (1970).

[3] I. F. Chang and S. S. Mitra, Phys. Rev. 172, 924 (1968).

[4] G. Lucovsky, M. H. Brodsky, and E. Burstein, Phys. Rev. B 2, 3295 (1970).

[5] M. H. Brodsky, G. Lucovsky, M. F. Chen, and T. S.

Plaskett, Phys. Rev. B 2, 3303 (1970).
[6]D. W. Taylor, Phys. Rev. 156, 1017 (1967).
[7]P. Soven, Phys. Rev. 156, 809 (1967).
[8]B. Velický, S. Kirkpatrick, and H. Ehrenreich, Phys. Rev. 175, 747 (1968); and P. N. Sen, Phys. Rev. (to be published).
[9]See, for example, M. Haas, H. B. Rosenstock, and R. E. McGill, Solid State Commun. 7, 1 (1969).
[10]D. W. Taylor, Solid State Commun. 13, 117 (1973).
[11]R. J. Elliott and D. W. Taylor, Proc. Phys. Soc. Lond. 83, 189 (1964).
[12]C. Kittel, *Introduction to Solid State Physics*, 4th ed. (Wiley, New York, 1971), p. 176ff.
[13]P. Mazur, E. W. Montroll and R. B. Potts, J. Wash. Acad. Sci. 46, 2 (1956); see also R. F. Wallis and A. A. Maradudin, Prog. Theor. Phys. 24, 1055 (1960).
[14]Proceedings of the Michigan State University Summer School on Alloys, edited by W. M. Hartmann and P. A. Schroeder (1973) (unpublished).
[15]R. D. Painter, thesis (Michigan State University, 1973) (unpublished).
[16]P. Dean [Rev. Mod. Phys. 44, 127 (1972)] gives a review of this work.
[17]R. D. Painter and W. M. Hartmann (unpublished); Bull. Am. Phys. Soc. 18, 777 (1973).
[18]E. Burstein, in *Phonons and Phonon Interactions*, edited by T. Bak (Benjamin, New York, 1964), p. 276ff.
[19]H. Harada and S. Narita, J. Phys. Soc. Jap. 30, 1628 (1971).
[20]M. P. Lisitsa, M. Ya. Valakh, and N. K. Konovets, Phys. Status Solidi, 34, 269 (1969).
[21]J. H. Fertel and C. H. Perry, Phys. Rev. 184, 874 (1969).
[22]F. Krueger, O. Reinkober, and E. Koch-Holm, Ann. Phys. (Paris) 85, 110 (1928).
[23]H. W. Verleur and A. S. Barker, Jr., Phys. Rev. 155, 750 (1967).
[24]H. W. Verleur and A. S. Barker, Jr., Phys. Rev. 149, 715 (1966).
[25]M. Ilegems and G. L. Pearson, Phys. Rev. B 1, 1576 (1970).